

We are IntechOpen, the world's leading publisher of Open Access books Built by scientists, for scientists

6,900

Open access books available

185,000

International authors and editors

200M

Downloads

Our authors are among the

154

Countries delivered to

TOP 1%

most cited scientists

12.2%

Contributors from top 500 universities



WEB OF SCIENCE™

Selection of our books indexed in the Book Citation Index
in Web of Science™ Core Collection (BKCI)

Interested in publishing with us?
Contact book.department@intechopen.com

Numbers displayed above are based on latest data collected.
For more information visit www.intechopen.com



Crack-Healing Ability of Structural Ceramics and Methodology to Guarantee the Reliability of Ceramic Components

Koji Takahashi, Kotoji Ando and Wataru Nakao
*Yokohama National University, Yokohama
Japan*

1. Introduction

The heat-resistant limit of structural ceramics is 1273K ~ 1773K, which is greatly superior to that of metallic material. Structural ceramics are a candidate element for high-temperature apparatuses such as gas-turbines and fusion reactors. However, the fracture toughness of ceramics is fairly low compared with metallic material, and the following problems have occurred. (1) Cracks occur by the usual machining process (grinding, polish, etc.), lowering the reliability. In order to prevent this, precise polishing is required in the final stage, which is time-consuming, and there are also problems with fabrication efficiency and fabrication cost (2) Crack sizes of about 10 ~ 30 μm in depth affect the reliability. The nondestructive-inspection technology for detecting cracks of 10 ~ 30 μm is underdeveloped. Therefore, the reliability of major parts is low. (3) There is a possibility that a crack will occur in the components while they are being used at higher temperatures, by whatever cause. When a crack occurs, the reliability is greatly lowered.

The options for resolving these problems are as follows. (a) Improve the fracture toughness of the material by such means as microstructure control and fiber reinforcement. (b) Conduct a nondestructive inspection before use, and detect and repair any dangerous cracks found. (c) Conduct a proof test to prevent use of a low reliability member. (d) Induce a self-crack-healing ability, so that all dangerous cracks can be healed. There are world-wide active investigations of options (a) to (c). In this chapter, special attention is paid to method (d), the self-crack-healing ability of structural ceramics.

There are three advantages to using a material that can heal surface cracks. (A) If the self-healing of the surface crack which exists is carried out after an efficient machine operation is performed, then there is a great advantage in fabrication efficiency and fabrication cost. (B) Since all surface cracks are healed, reliability improves greatly. (C) It is advantageous if a crack which occurs while in service can be healed and full recovery of strength achieved.

From the above ideas, the self-crack-healing behaviors of ceramics were investigated by Ando and co-worker. Silicon nitride (Ando et al, 1998; Yao et al., 2001), alumina (Takahashi et al., 2003; Ando et al., 2004; Nakao et al., 2005a), and mullite (Chu et al., 1995; Nakao et al., 2006), SiC (Kim Y.W. et al., 2003; Lee et al., 2005a) and ZrO₂ (Houjou et al., 2010), with the self-crack-healing ability have been developed. In the following section, an outline is given of the crack-healing behavior of ceramics.

2. Nano-composite and multi-composite

The nano-composite material has the following specificity (Niihara, 1991; Ando et al., 2004) .

1. SiC particles of nano size are added to the material, preventing grain growth of the matrix in the sintering process, and improving the bending strength through grain refinement: For example, in the case of an alumina, bending strength can be increased from about 400 MPa to 700 ~ 1000 MPa (Ando et al., 2004).
2. SiC particles of nano size 15 to 30 vol% added to the material, and induce a self-crack-healing ability.
3. SiC particles of nano size are distributed not only in the grain boundaries of an alumina, but in individual grains and increases the heat-resistant limit by 300 K.

The fracture-surface photography of the Al_2O_3 nano-composite material is shown in Fig 1. Most of the SiC particles were distributed uniformly in the grain boundaries; however, several nanosized SiC particles were distributed in the Al_2O_3 grain, as shown in Fig. 1 (Ando et al., 2004).

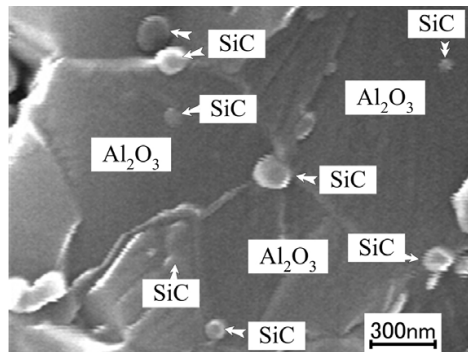


Fig. 1. Microstructure of Al_2O_3 / 15 vol% SiC particles nanocomposite

A multi-composite material is a material which combines nanosized SiC particles and SiC whiskers in the proportion of 25 to 30%, and has excellent self-crack-healing ability, fracture toughness, strength (Nakao et al., 2006, Takahashi et al., 2007). The proportion fraction of SiC particles to SiC whiskers is determined by taking into consideration the self-crack-healing ability and fracture toughness requirements. If the proportion fraction of SiC particles is increased, then the crack healing rate will be increased. If the proportion fraction of SiC whiskers is increased, then the fracture toughness will be improved (Nakao et al., 2005a).

The composition system of the ceramics used in this paper and the effective temperature ranges in which crack-healing is possible are shown in Table 1. The room-temperature bending strength and fracture toughness of the multi-composite ceramics are shown in Table 2.

It has been common knowledge for many years that the strength of ceramics is improved by heat-treatment in air. This occurs by three mechanisms, as follows.

- i. The crack-healing phenomena, which is explained in this paper.
- ii. Re-sintering.
- iii. Release of tensile residual-stress.

In case ii), the material must be heated to a nearly sintering temperature, which is a higher temperature than it is heated in the crack-healing phenomena (Lange et al., 1970; Kim et al., 2003). In case iii), the strength recovery rate is small and the crack still remains (Thompson et al., 1995).

The material with a self-crack-healing ability described in this paper has all of the following attributes.

1. The material itself detects an occurrence of a crack and begins crack-healing activities.
2. A crack causes a 50 ~ 90 % reduction in the strength of a material, but in material with a self-crack healing ability, the material heals the crack completely, and the strength of the material is completely recovered.
3. The strength of a crack-healed area is equivalent to or higher than that of a matrix area up to about 1673 K.

Materials	Effective Temperature Range for crack-healing			
Si ₃ N ₄ / 20 vol% SiC particles composite (8 wt% Y ₂ O ₃)	1073	—	1573	K
Al ₂ O ₃ / 15 vol% SiC particles composite	1173	—	1573	K
Mullite/ 15 vol% SiC particles composite	1273	—	1473	K
SiC sintered with Sc ₂ O ₃ and AlN	1473	—	1673	K

Table 1. Effective temperature range of self-crack-healing for several ceramics

Sample name	Content				Strength (MPa)	Fracture Toughness (MPam ^{1/2})
	Alumina	Mullite	SiC Particle (Diameter:0.27 μ m)	SiC Whisker (Diameter:0.8-1.0 μ m, (Length:30-100 μ m)		
AS15P	85		15		850	3.2
AS30P	75		30		1050	3.6
AS20W	80			20	970	4.8
AS30W	70			30	830	5.8
AS20W10P	70		10	20	980	5
MS15P		85	25		470	2.2
MS15W		85		15	710	2.8
MS20W		80		20	840	3.6
MS25W		75		25	820	4.2
MS15W5P		80	5	15	750	3.2
MS15W10P		75	10	15	740	3.5

Table 2. Strength and fracture toughness of Al₂O₃ and Mullite reinforced by SiC particles and Whiskers

3. Nano-composite and multi-composite

3.1 Mechanism of crack healing

The crack healing of ceramics developed by the authors is caused by the following oxidation reaction of SiC.



From Eq.(1), it can easily be understood that a monolithic mullite or a monolithic alumina does not reveal a crack healing ability, since oxidization is saturated in these materials. A schematic diagram of the crack healing mechanism is shown in Fig 2. The following three conditions must be met for a crack-healed area to recover completely.

- i. The volume between the crack walls must be completely filled with the products formed by the crack-healing reaction:
- ii. The strength of the crack-healing substance must be equivalent to or higher than that of the matrix:

There is a glass phase and a crystalline phase in SiO_2 in Eq.(1). If the crack-healing material was crystal SiO_2 , then the crack-healed sample would exhibit high bending strength even at an elevated temperature. However, if the crack-healing material was glassy SiO_2 , then the crack-healed sample would exhibit low bending strength at an elevated temperature. A key point of crack-healing technology is how many crystalline phases are deposited in a crack-healing substance. The large exothermic heat of 943 kJ in Eq. (1) seems to satisfy this condition.

- iii. The crack healing substance must be strongly bonded to a matrix.

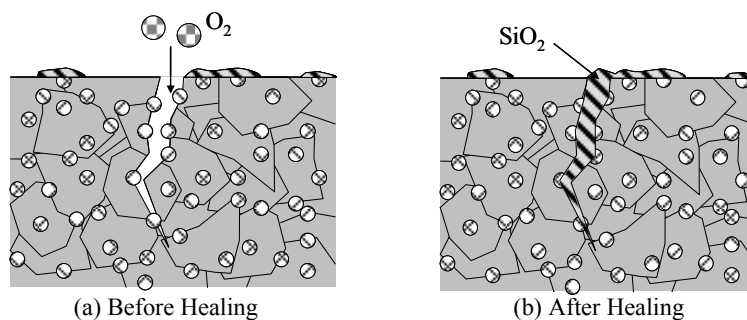


Fig. 2. Schematic illustration of crack-healing mechanism

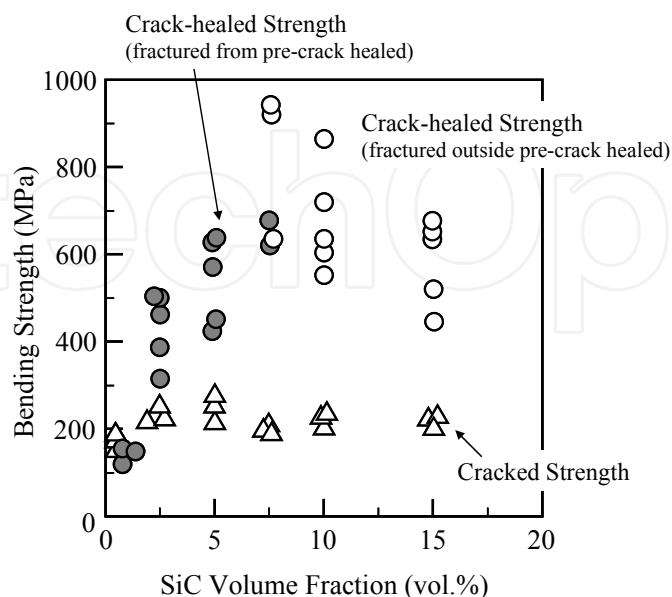


Fig. 3. Crack-healed and cracked strength of a $\text{Al}_2\text{O}_3/\text{SiC}$ composites as a function of SiC volume fraction

Bonding to a matrix is attained by the huge exothermic heat of 943 kJ by fusion and mixture of a matrix and a healing substance. How much nano size SiC should be added to the Al_2O_3 matrix in order to satisfy the three crack-healing conditions? We investigated the effect of the volume fraction of SiC on the crack-healing behavior of an $\text{Al}_2\text{O}_3/\text{SiC}$ composite.

Figure 3 shows the experimental results. The crack introduced on the test specimen is a semi-elliptical crack 100 μm in surface length and 45 μm in depth (hereafter called a standard crack). The open circles show the fracture of the specimens initiated from outside the crack-healed zone, indicating that complete crack healing occurred. With respect to strength, the optimal volume fraction of SiC is 7.5 to 10 %. However, with respect to crack-healing ability, a volume fraction of SiC larger than 10 % is recommended. However, when the SiC additive rate exceeds 30%, the strength begins to vary greatly, since a SiC agglomeration is formed. On the other hand, a large crack can be healed with an increased SiC volume fraction. The authors recommend a standard SiC volume fraction of 15 ~ 30 %.

3.2 Oxygen partial pressure and temperature dependency of crack-healing behavior

We used three-point bending-test specimens as shown in Fig 4 to evaluate the bending strength (σ_B) of a crack-healed specimen. We introduced the standard crack into the central part of the test specimen. The decreasing rate of the strength by this crack was 50 to 85%, although it was greatly dependent on the fracture toughness of the material.

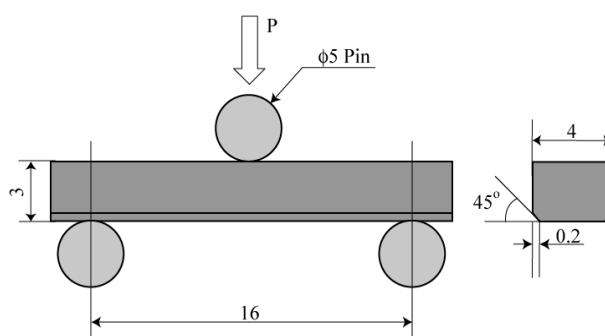


Fig. 4. Dimensions of three point bending specimens

The influence of atmosphere on the crack-healing behavior of $\text{Al}_2\text{O}_3/15 \text{ vol}\% \text{ SiC}$ is shown in Fig 5 (Kim B.S. et al., 2003). The bending strengths (σ_B) of a as-received test specimen are about 650 MPa. When a standard crack was introduced into this specimen, the σ_B was reduced to 180MPa and the decreasing rate of σ_B was about 73 %. However, when the crack healing of this pre-cracked specimen was carried out in air at 1573K for 1 h, the bending strength (σ_B) was improved up to about 800 MPa. The σ_B of a crack-healed specimen is larger than the σ_B of a as-received specimen. The reason for this is because even minute cracks on the surface of the as-received specimens recovered completely. However, when the pre-cracked specimens were heated in a vacuum, N_2 gas, and argon gas, the σ_B recovered to at most 350 MPa. The recovery of σ_B is insufficient. The slight increase of σ_B by this heat-treatment occurred because the tensile residual-stress of the crack tip was removed. Similar crack healing and strength recovery behaviors were reported in mullite (Chu et al., 1995), Al_2O_3 (Chou et al., 1998) and Si_3N_4 (Ando et al., 1998; Jung et al., 2008a). Figure 6 shows a specimen after the bending test. Fig 6 (a) shows the case of a pre-cracked specimen. The pre-cracked specimens fractured from the pre-crack division. In the case of Fig 6 (b), because a crack was healed completely, the crack was initiated from matrix division.

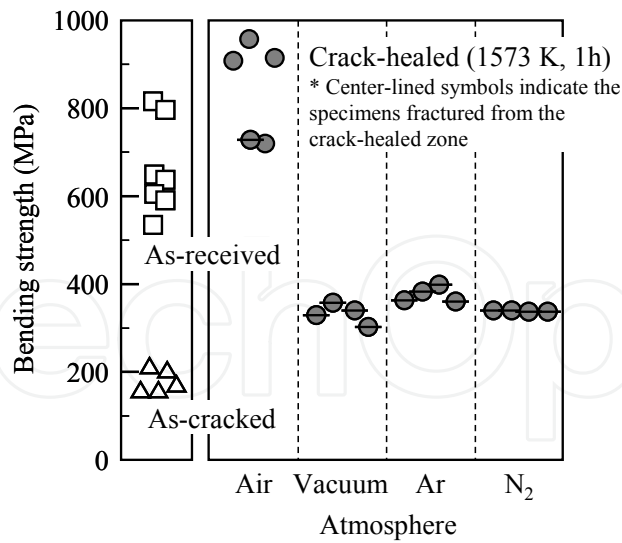


Fig. 5. Crack-healing behavior of alumina / 15 vol% 0.27 μm SiC particles composite under several atmospheres

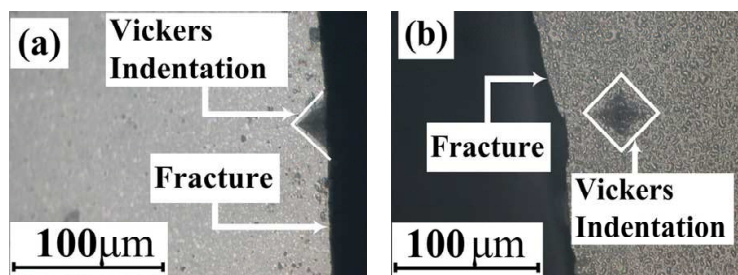


Fig. 6. Fracture initiation of Al_2O_3 / 15 vol% SiC particles composite (a) as-cracked (b) crack-healed at 1573 K for 1 h in air, from that one can find that pre-crack healed is stronger than the other part

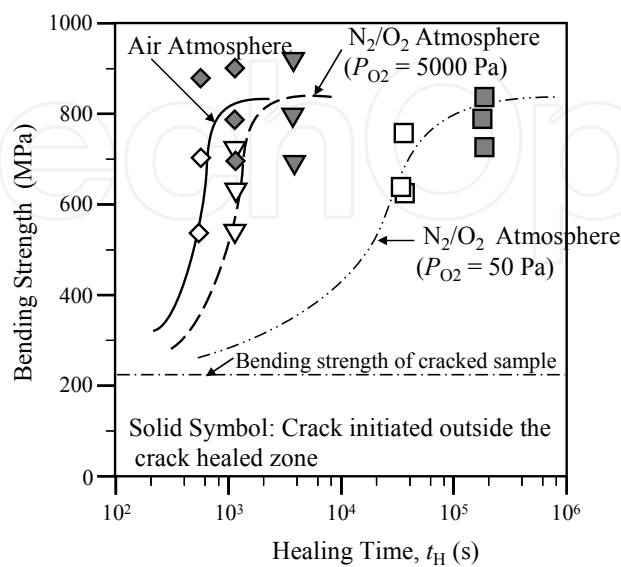


Fig. 7. Effect of partial oxygen pressure on crack healing behavior at 1673K

As described in section 3.1, crack healing is dependent on an oxidation reaction. Therefore, it is assumed that crack-healing behavior is greatly dependent on oxygen partial pressure. The influence of oxygen partial pressure on crack-healing behavior is shown in Fig 7, in $\text{Al}_2\text{O}_3/\text{SiC}$ composite materials (Osada et al., 2009). When crack-healing was carried out at 1673K, in air (oxygen partial pressure: 21kPa), the crack healed completely in about 20 minutes. When the oxygen partial pressures were 5000 and 50 Pa, the crack healed completely in about 1 h and 70 h, respectively. Moreover, the test specimen which healed in thin oxygen showed a bending strength equivalent to a matrix division to 1673K. It is said that the oxygen partial pressure in the exhaust gas of a gas-turbine or a vehicle is about 8kPa-10kPa, which is approximately half in an atmosphere. So it is anticipated that the surface crack can be healed in oxygen partial pressure in the exhaust gas of a gas-turbine or a vehicle.

The influence of temperature on crack-healing behavior is shown in Fig 8 (Ando et al., 2009; Nakao et al., 2009). When the crack-healing times were 10 h and 300 h, the temperatures in which a crack was healed completely were about 1473 K and 1273 K, respectively. By conducting an experiment as shown in Fig 8 on various materials, we found the shortest time t_{HM} which can heal a crack completely from a certain temperature T_{HL} . Fig 9 shows the Arrhenius plot of the experimental result. The relationship between $1/t_{\text{HM}}$ and $1/T_{\text{HL}}$ can be shown by the Arrhenius equation as follows (Ando et al., 2002a).

$$\frac{1}{t_{\text{HM}}} = Q_0 \exp\left(\frac{-Q_{\text{H}}}{RT_{\text{HL}}}\right) \quad (2)$$

The activation-energy (Q_{H}) and proportional moduli (Q_0) of each material were calculated from Fig. 9. The result is shown in Table 3. By using Table 3, the relationship between the time (t_{HM}) required to heal a standard crack completely and the crack-healing temperature can be estimated. However, Eq. (2) is applicable in $t_{\text{HM}} = 1 \text{ h} \sim 300 \text{ h}$.

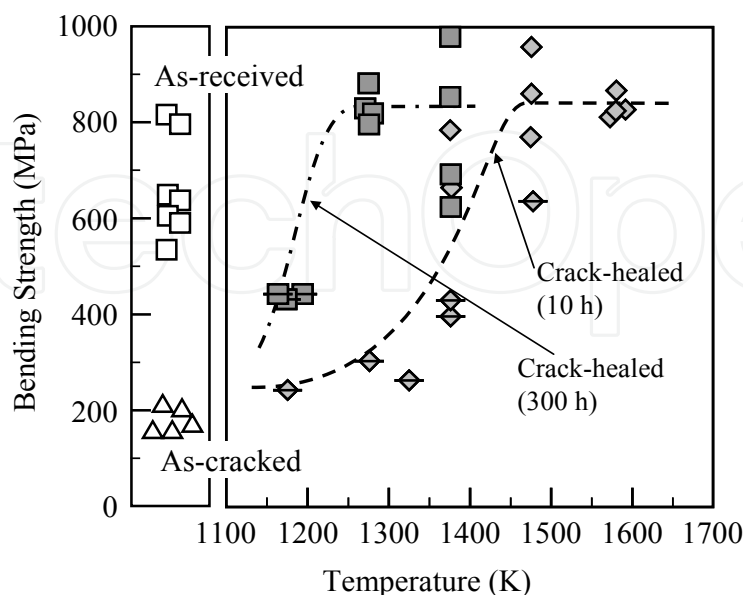


Fig. 8. Relationship between crack-healing temperature and strength recovery for $\text{Al}_2\text{O}_3/15$ vol% SiC particles composite

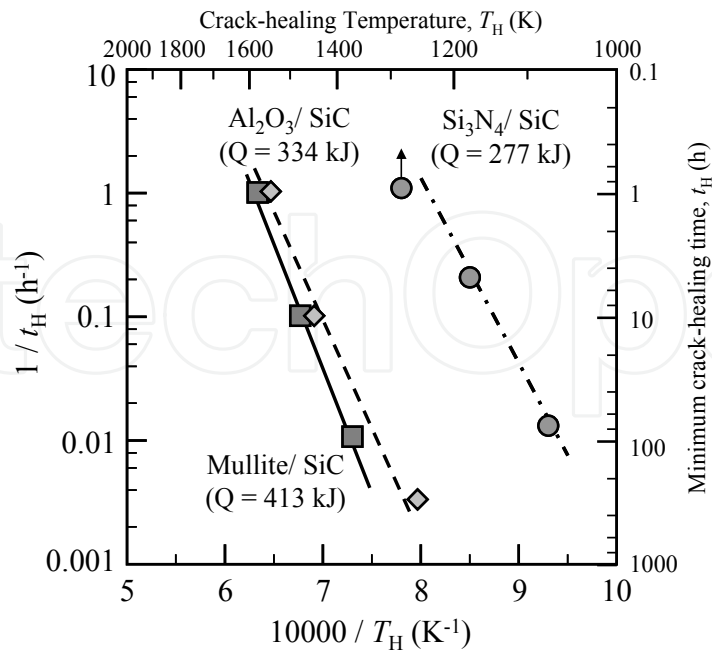


Fig. 9. Arrhenius plots on the crack-healing of several ceramics having crack-healing ability

Material	Activation Energy Q_H (Kj/mol)	Proportional Coefficient Q_0 (1/hour)
Si_3N_4/SiC	277	4.2×10^{11}
Si_3N_4	150	5.3×10^4
Al_2O_3/SiC	334	1.7×10^{11}
Mullite/SiC	413	4.7×10^{23}

Table 3. Active energy and proportional coefficient for crack-healing

3.3 Crack-length dependency of crack-healing behavior and strength

The crack-length dependency of a fracture stress or a crack-healing behavior is important. The crack-length dependency of a fracture stress or a crack-healing behavior obtained with Al_2O_3 strengthened with SiC whiskers is shown in Fig 10 (Nakao et al., 2005a). The crack-healing conditions are 1673K and 1h in air. The $2c$ in Fig. 10 is the surface length of a semi-elliptical crack. The aspect ratio of a crack is about 0.9. The open triangles are the bending strength (σ_B) of a pre-cracked specimen, and the solid circles are the bending strength of a crack-healed specimen. When the pre-crack length was less than 250 μm , the specimens recovered bending strength nearly completely and fractured from the matrix division except for one example. This result showed that the pre-crack length in which crack healing is possible is about 250 μm . In addition, with the material shown in Table 1 and Table 2, the pre-crack length in which crack healing is possible is about 250 μm , as in the case of Fig 10.

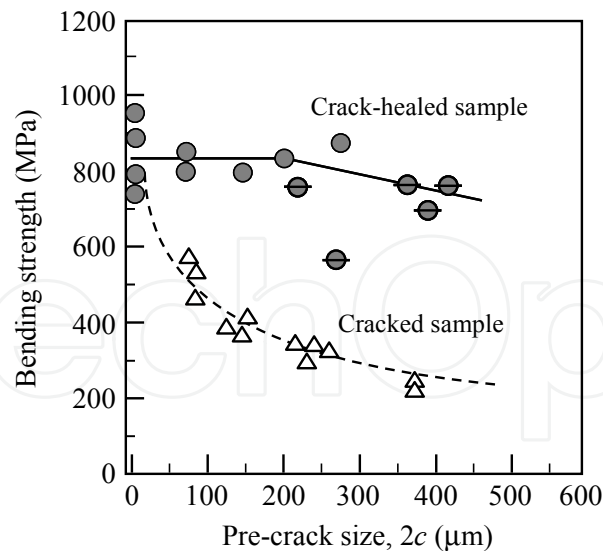


Fig. 10. Bending strength of the crack-healed Al_2O_3 / 30 vol% SiC whiskers composite as a function of surface length of a semi-elliptical crack

4. High-temperature strength characteristic of crack-healed specimen

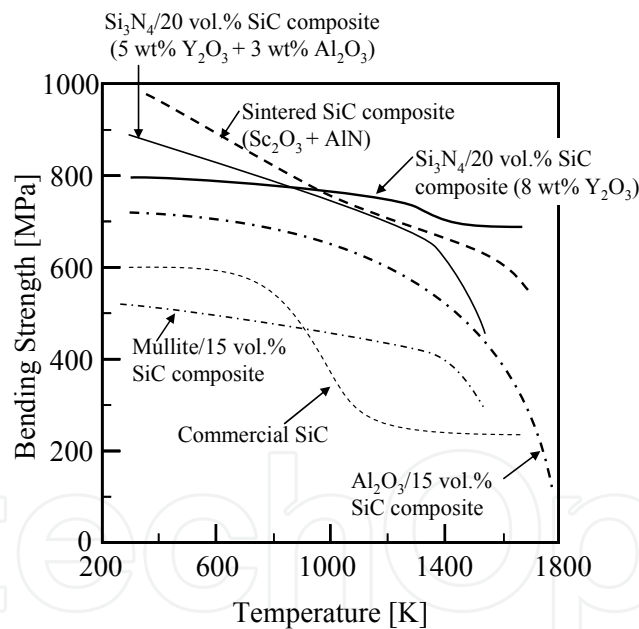


Fig. 11. Temperature dependences of the bending strength of the typical several ceramics crack-healed

The temperature dependency of the bending strength (σ_B) of a crack-healed specimen is shown in Fig 11. Each test specimen was crack healed by an optimum condition after a standard crack was introduced. The heat resistance limit for the bending strength of $\text{Al}_2\text{O}_3/\text{SiC}$ is about 300 K higher than that of monolithic Al_2O_3 ; this excellent increase in the heat resistance limit was attained by a nano-composite, as mentioned in section 2. The heat-resistant limit at the crack-healed division of the commercial SiC was 873K, much lower than that of the matrix division (Lee et al., 2005b). As shown in the figure, a new SiC, which

has a heat-resistant limit of a crack-healed division of about 1673K, has been developed, and we examined its usage (Lee et al., 2005a). The heat-resistant limit of the silicon-nitride with Al_2O_3 added to it was about 1273K. The heat-resistant limit of the new silicon nitride which improves the composition system is about 1673K, which is higher than the heat-resistant limit of the silicon nitride with Al_2O_3 added. The large improvement in such a heat-resistant limit was attained by the crystallization of a grain boundary or a crack-healing substance. In addition, most test specimens fractured from the matrix division below to the heat-resistant limit temperature among the materials of Fig. 11, except the commercial SiC. This implied that the crack-healing division had sufficient bending strength.

5. Crack-healing behavior of machined specimens

In general, final machining processes such as polishing and lapping are performed to remove non-acceptable flaws. Although these processes are generally very costly, they cannot eliminate minute cracks. Moreover, even if final machining is adopted, a minute crack may remain, causing a reliability problem. It is anticipated that substituting the crack-healing process for the final machining processes leads to economical manufacturing of ceramic components with high reliability. The crack-healing behavior of machined specimens was investigated by several researchers (Lee et al., 2005c; Osada et al., 2007; Jung et al., 2008b). The experimental results showing the effects of crack-healing on increasing the reliability of machined components will be explained (Osada et al., 2007).

Machined $\text{Al}_2\text{O}_3/20$ vol.% SiC whiskers having a semicircular groove were used. The sintered plates were cut into 3 mm × 4 mm × 22 mm rectangular bar specimens. A semicircular groove was made at the center of the smooth specimens by using a diamond-coated ball-drill as shown in Fig. 12. The cut depth by one pass (d_c) during machining of the semicircular groove was $d_c = 5 \sim 15 \mu\text{m}$.

All fracture tests were performed on a three-point bending system with a span of 16 mm, as shown in Fig. 12. The crosshead speed was 0.5 mm/min. The tests were conducted at room temperature. The local fracture stresses (σ_{LF}) considering the stress concentration factor of the semicircular groove ($\alpha = 1.2$) were evaluated.

Figure 13 shows the strength of the machined specimens with a semicircular groove as a function of the cut depth by one pass (d_c). The open triangle symbols show the local fracture stress (σ_{LF}) of the as-machined specimen. The σ_{LF} of the as-machined specimens decreased with increasing d_c . This behavior was caused by the fact that the crack depth caused by machining increased with increasing d_c . The as-machined specimens always fractured from the surface cracks caused by machining, as shown in Fig. 14. Figure 14 shows the scanning electron microscope (SEM) images of the fracture surface of the as-machined specimen. The dashed lines in Fig. 14 indicate the crack front. As shown in this figure, these surface cracks acted as the fracture initiation. Thus, the σ_{LF} of the as-machined specimens decreased compared with the healed smooth specimens. The open square symbols in Fig. 13 show the σ_{LF} of the machined specimen healed at 1673 K for 10 h in air. The σ_{LF} of these specimens increased significantly by crack healing. The σ_{LF} of the machined specimens was almost equal to the fracture stress of the healed smooth specimens (solid circles). Thus, the surface cracks introduced by the machining process were healed.

Therefore, it was concluded that crack healing could be an effective method for improving the structural integrity of machined alumina and reducing machining costs.

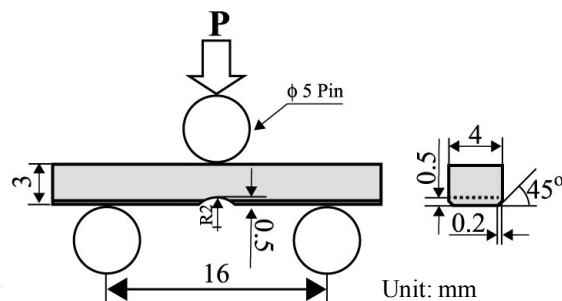


Fig. 12. Schematics of machined specimen

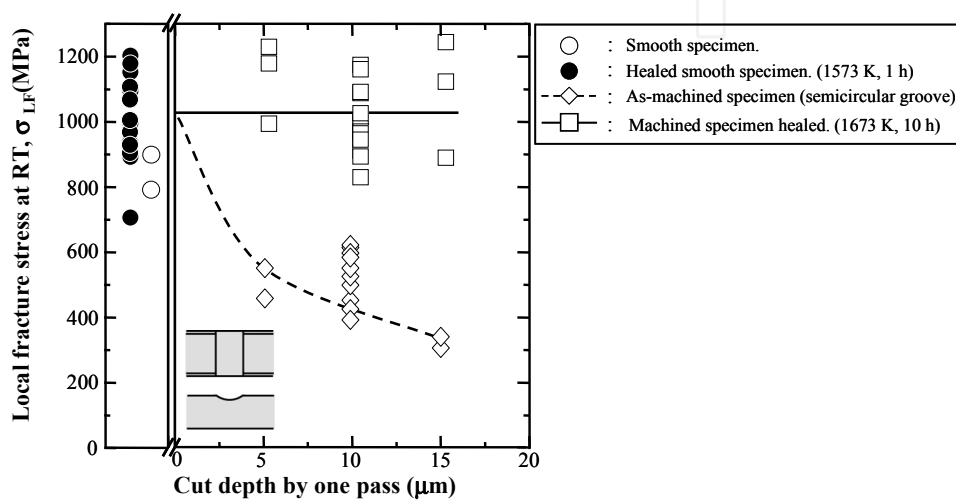


Fig. 13. Effect of depths of cut by one pass on the local fracture stress at room temperature of the machined specimens healed

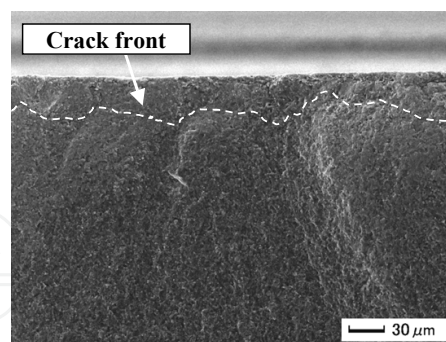


Fig. 14. SEM images of fracture surface of as-machined specimen

6. Crack-healing behavior during service

Ceramic components are often operated continuously under constant or cyclic loading at elevated temperatures under lower oxygen partial pressure. If a crack initiates during service, the component's reliability will be considerably reduced. If the crack could be healed under even service conditions, and the healed zone had sufficient strength, the reliability and lifetime of ceramic components could be increased. The crack-healing behaviors under constant or cyclic stress have been systematically studied for $\text{Si}_3\text{N}_4/\text{SiC}$

(Ando et al, 2002b; Takahashi et al., 2005), Mullite/SiC (Ando et al., 2001; Takahashi et al. 2007), Al₂O₃/SiC (Nakao et al., 2005b), and SiC (Lee et al., 2005a). Pre-cracks of 100 μm can be healed completely, even under constant or cyclic stress.

To take advantage of the crack-healing ability during service, it is essential to determine the threshold stress for crack-healing below which a crack can be completely healed. In this section, the critical stress condition for crack healing in Si₃N₄/SiC and other ceramics are shown.

6.1 Crack-healing behavior of Si₃N₄/SiC under stress and low oxygen pressure

The material studied was a hot-pressed SiC-particle reinforced Si₃N₄ that contained 20 wt% SiC particles and 8 wt% Y₂O₃ as a sintering additive. Semi-circular surface cracks of 100 μm in surface length were introduced at the center of the tensile surface of the bending test specimens using a Vickers indenter. After introduction of the pre-cracks, crack-healing tests under cyclic or constant stress were carried out. Figure 15 shows the crack-healing process. Crack-healing was carried out under cyclic ($\sigma_{\max, ap}$) or constant (σ_{ap}) bending stresses at a healing temperature (T_h) for a prescribed healing time (t_h). After the crack-healing process, the bending strengths of the specimens were measured at room temperature in air.

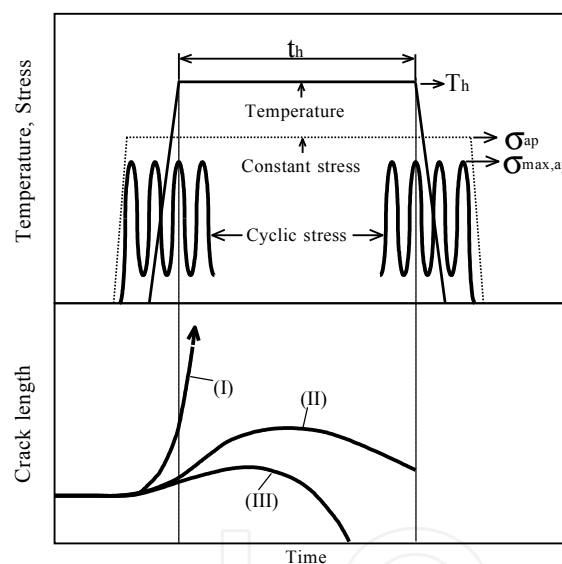


Fig. 15. Schematic illustration of crack-healing under stress and crack growth behaviors

Figure 16 shows the results of the bending tests on specimens crack-healed at 1473K for 5h under constant stress in $P_{O_2}=500$ Pa (Takahashi et al., 2010). The solid triangles represent the bending strengths of the crack-healed specimens. Open triangle symbols indicate the bending strengths of the pre-cracked specimens. The asterisks indicate specimens that fractured outside the crack-healed zone, suggesting that the pre-cracks were healed completely. The threshold stresses for crack-healing were defined as the maximum stresses below which the crack-healed specimens recovered their bending strengths and below which most specimens fractured outside the crack-healed zone. The specimens crack-healed under a constant stress of 200 MPa showed quite high bending strength, comparable to that of the specimens crack-healed under no stress. Most of the specimens crack-healed under 200 MPa fractured outside the crack-healed zone. However, the specimens crack-healed under a constant stress of 250 MPa showed low bending strength and fractured from the

crack-healed zone. Therefore, the threshold stress for crack-healing in air was determined to be 200 MPa. These results indicate that complete strength recovery could be achieved by crack-healing even under service conditions, i.e., with an applied stress below $\sigma_{app.}=200$ MPa and an oxygen partial pressure over $P_{O_2} = 500$ Pa.

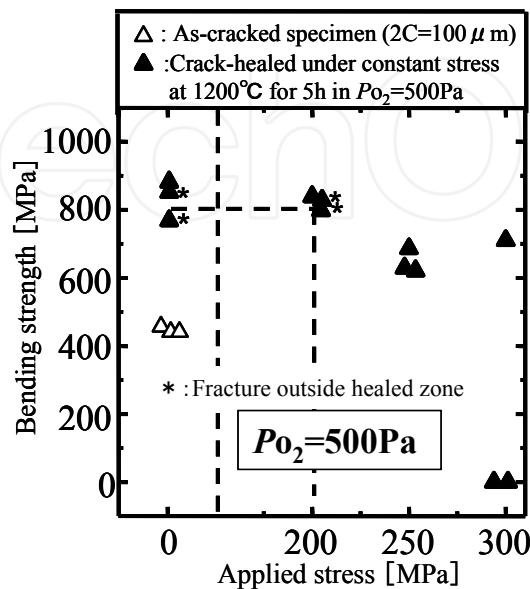


Fig. 16. Room temperature bending strength of crack-healed specimen as a function of applied stress during crack-healing in $P_{O_2}=500$ Pa at 1473K. (Si_3N_4/SiC)

Figure 17 shows the bending strength (σ_B) and cyclic fatigue limit (σ_{f0}) at the healing temperatures between 1173 K and 1473 K. The ratio of σ_{f0}/σ_B was 0.67 ~ 0.86 at each healing temperature (Takahashi et al., 2005). Therefore, it can be concluded that the cyclic fatigue limit was sufficiently high even at the healing temperature.

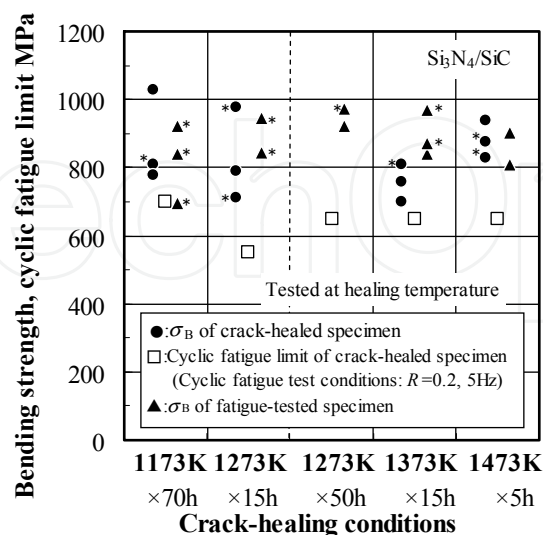


Fig. 17. Results of bending tests and cyclic fatigue tests of Si_3N_4/SiC at healing temperatures between 1173 K and 1473 K. Cyclic stress during crack-healing: $\sigma_{max} = 210$ MPa, $R = 0.2$ and $f = 5$ Hz. Asterisk indicate that fracture occurred outside of the crack-healed zone

On the bottom of Fig. 15, the crack-healing behaviors under stress are indicated schematically (Takahashi et al., 2005). The change in the crack-length during crack-healing is divided into three cases, (I), (II) and (III). In process (I), slow crack growth from the pre-crack tip occurs and the cracks lead the specimen to failure because the crack growth rate is higher than the crack-healing process. In process (II), slow crack growth from the pre-crack tip also occurs. The crack-healing process starts at high temperature, the crack growth rate decreases due to crack-healing and finally the cracks are healed. In process (III), slow crack growth from the pre-crack does not occur, and thus the pre-cracks are easily healed.

In the case of crack-healing under the constant bending stress (σ_{ap}) of 250 MPa and 300 MPa, the crack-healing behavior is classified into process (I) or (II). However, in the case of σ_{ap} = 200 MPa, the crack-healing behavior is classified into process (III). The applied stresses are lower than the threshold stress for crack-healing and the pre-cracks were healed easily.

6.2 Threshold stress for crack-healing for $\text{Al}_2\text{O}_3/\text{SiC}$ and Mullite/SiC

Figure 18 shows the threshold constant or cyclic stress for crack healing as a function of the bending strength of pre-cracked specimens (Nakao et al., 2007). $\text{Al}_2\text{O}_3/15 \text{ vol}\% \text{ SiC}$ particles (AS15P), $\text{Al}_2\text{O}_3/15 \text{ vol}\% \text{ SiC}$ whiskers (AS15W), mullite/15 vol% SiC particles (MS15P), and mullite/15 vol% SiC whiskers (MS15W) were tested. The closed and open symbols indicate the threshold constant and cyclic stresses, respectively. All data except that of MS15W are satisfied by the proportional relation in spite of the different crack-healing conditions. The proportional constants for the relationship between the threshold stress and bending strength of pre-cracked specimens is 64 % for constant stress and 76 % for cyclic stress.

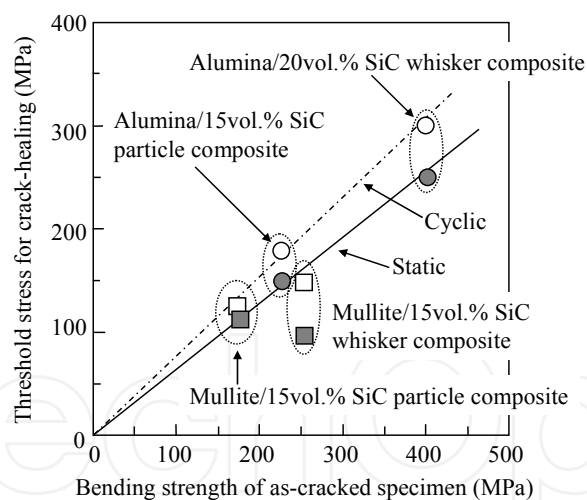


Fig. 18. Relation between threshold stress during crack-healing and the fracture strength for the corresponding as-cracked specimens

7. A methodology to increase the structural integrity against embedded flaws

Oxygen is necessary for crack-healing, and thus embedded flaws such as pores and abnormally large grains cannot be healed. These facts suggest the importance of a proof test for higher reliability. However, engineering ceramics show nonlinear fracture behavior as shown in Fig. 19, and ceramics components are not used only at the proof-tested temperatures. Ando et al. have proposed a theory to evaluate the temperature dependence of a guaranteed

(minimum) fracture stress of a proof-tested sample based on nonlinear fracture mechanics (Ando et al., 2002c). In this section, the theory and its application are explained.

The nonlinear fracture behavior is expressed very well by the process zone size failure criterion, as shown in Fig. 19 proposed by Ando et al (Ando et al., 1993). The criterion is expressed by eq. (3) as follows:

$$D_C = \frac{\pi}{8} \left(\frac{K_{IC}}{\sigma_0} \right)^2 = a_e \left\{ \sec \left(\frac{\pi \sigma_C}{2 \sigma_0} \right) - 1 \right\} \quad (3)$$

where D_C is the critical process zone size, σ_C and σ_0 are the fracture stress of the as-cracked specimen and the plain specimen (intrinsic bending strength), respectively, K_{IC} is the plane strain fracture toughness and a_e is the equivalent crack length.

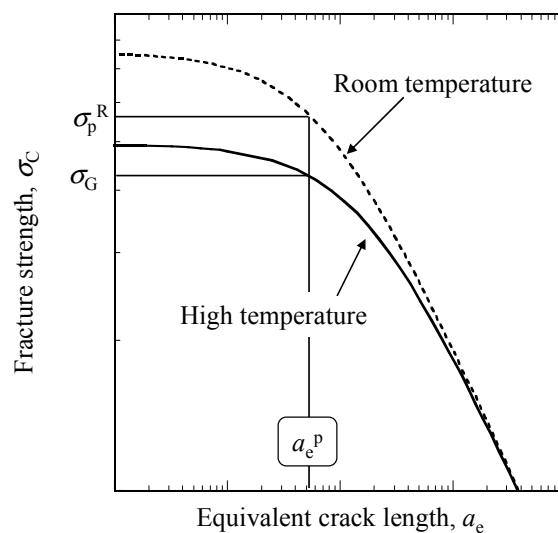


Fig. 19. Schematic illustration of proof-test theory and the effect of equivalent crack on fracture strength at room temperature and high temperature

Figure 19 shows a schematic relationship between σ_C and a_e . The dotted line and solid line show the relationship between σ_C and a_e at room temperature and high temperature, respectively. If the proof test is carried out at room temperature, the maximum residual equivalent crack size, a_e^p , can be expressed by eq. (4):

$$a_e^p = \frac{\pi}{8} \left(\frac{K_{IC}^R}{\sigma_0^R} \right)^2 \left\{ \sec \left(\frac{\pi \sigma_p^R}{2 \sigma_0^R} \right) - 1 \right\}^{-1} \quad (4)$$

where σ_p^R is the proof test stress at room temperature, and the superscript R indicates the value at room temperature. Since embedded flaws cannot be healed, the value of a_e^R is not changed in spite of the crack-healing treatment. Thus, the σ_G can be expressed as follows by expanding eq. (5) with regard to room temperature and high temperature:

$$\sigma_G = \frac{2 \sigma_0^T}{\pi} \arccos \left\{ \left(\frac{K_{IC}^T}{K_{IC}^R} \right)^2 \left(\frac{\sigma_0^R}{\sigma_0^T} \right)^2 \left\{ \sec \left(\frac{\pi \sigma_p^R}{2 \sigma_0^R} \right) - 1 \right\} + 1 \right\}^{-1} \quad (5)$$

where the superscript T indicates the value at elevated temperature T . By obtaining the temperature dependence of K_{IC} and σ_0 , one can estimate σ_G .

Figure 20 shows the data on the fracture stress of the crack-healed and the proof-tested specimens as a function of temperature with the evaluated σ_G for the crack-healed alumina/20 vol% SiC particles composite when $\sigma_p = 435$ MPa (Ono et al., 2007). Except the data at 1373 K, all specimens have higher strength than the σ_G at all temperatures. Also, the minimum values of the experimental fracture stress are almost equal to the σ_G at all temperatures. At 1373 K, the σ_{Fmin} is 6.8 % less than σ_G , but the value exists in the dispersion evaluated from the K_{IC} and the σ_0 that have large scatters.

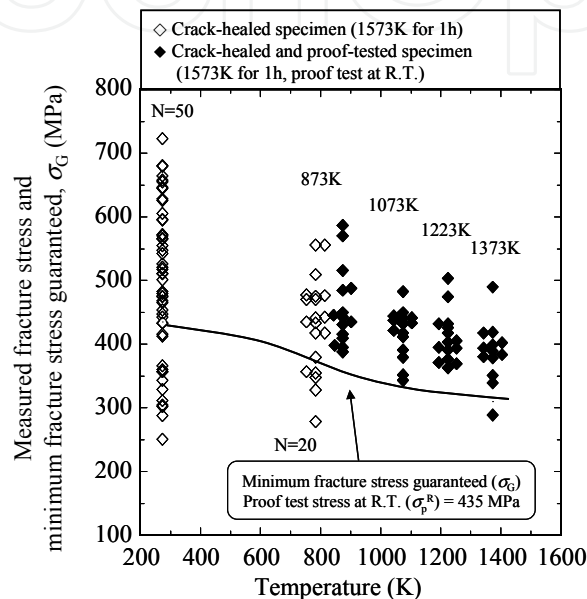


Fig. 20. Fracture stress of the crack-healed and proof tested specimens as a function of temperature with the evaluated minimum fracture stress guaranteed of the crack-healed $Al_2O_3/20$ vol.% SiC particles composite proof tested under 435 MPa

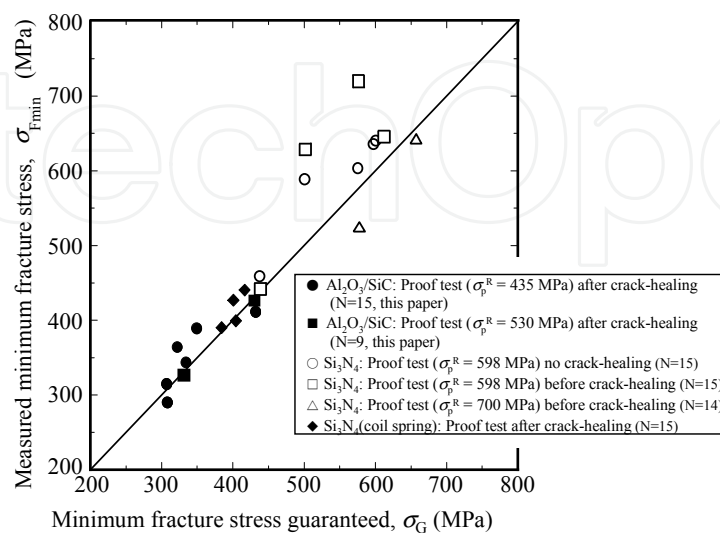


Fig. 21. Comparison between minimum fracture stresses guaranteed and measured minimum fracture stress

Moreover, the guaranteed theory can be applied to Si_3N_4 (Ando et al., 2002b; Ando et al., 2005) and coil spring made of Si_3N_4 (Nakatani et al., 2005). The results obtained can be seen in Fig. 21, where the measured $\sigma_{F\min}$ is plotted as a function of the evaluated σ_G . N in the figure denotes the number of samples used to obtain $\sigma_{F\min}$. Four solid diamonds indicate the data on the ceramic coil spring made of silicon nitride. All $\sigma_{F\min}$ showed good agreement with σ_G . From this figure, it can be concluded that eq. (5) can be applied to $\text{Al}_2\text{O}_3/\text{SiC}$, Si_3N_4 , and even to a coil spring.

8. Through life reliability of ceramic components

The flow chart of a new methodology to guarantee the structural integrity of a ceramic component is shown in Fig. 22. This new concept consisted of the following three stages: (a) crack-healing under optimized conditions, (b) proof testing, and (c) in-situ (in-service) crack-healing.

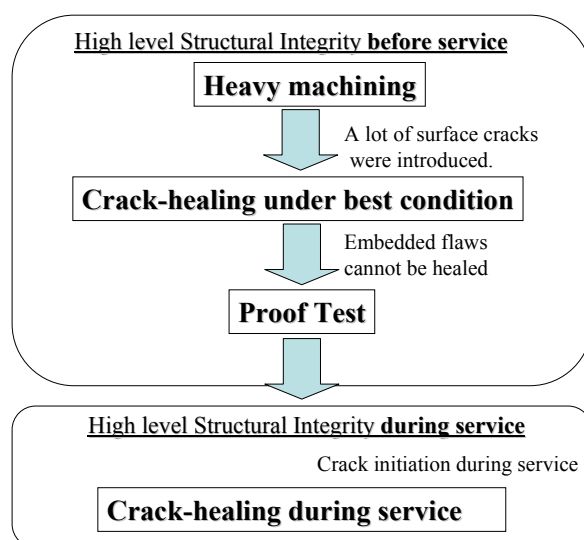


Fig. 22. Through life reliability management of ceramic component using crack-healing and proof test

By machining, many surface cracks will be induced and reliability will decrease considerably. However, by crack-healing under optimized conditions, surface cracks can be healed completely and reliability will be increased.

However, for the crack-healing of the above ceramics, oxygen is necessary. Consequently an embedded flaw cannot be healed. This means that the structural integrity of ceramic components before service cannot be guaranteed only by crack-healing technology. A new theory to explain the temperature dependence of minimum fracture stress guaranteed based on non-linear fracture mechanics was proposed as mentioned in section 7. Thus, before service, the structural integrity of ceramic components can be confidently guaranteed using the concept: crack-healing + proof test.

After service, if a crack is initiated, structural integrity will decrease considerably depending on the crack size. However, if a material can heal a crack in service, it would be very desirable for structural integrity. As mentioned in section 6, several materials developed by the present authors can heal a crack during service. Thus, a new concept shown in Fig. 22 is effective to increase the through life reliability of ceramic components.

9. Conclusion

Structural ceramics are generally brittle, which seriously affects the reliability of ceramic components. Four methods are used to resolve this weakness: (a) the ceramic is toughened by fiber reinforcement or microstructural control, (b) high level non-destructive inspection and repair of the unacceptable flaws, (c) using the proof test and then only using the components that have high reliability, and (d) making use of the self-crack-healing ability. In this chapter, special attention was paid to method (d), the self-crack-healing ability of structural ceramics.

In Section 1, the advantages of using the crack-healing ability of ceramics are outlined. In Section 2, nano-composite and multi-composite materials having crack-healing ability are presented. In Section 3, basic crack-healing ability is introduced in detail. In Section 4, the high-temperature strength characteristics of crack-healed specimens are explained. Machining is a necessary process for ceramic machine components, but machining can cause many cracks in the components. In Section 5, it is explained in detail how the many cracks introduced by machining can be healed and strength recovered completely. If a material were able to heal a crack that initiated during its service, it would be extremely beneficial for the structural integrity of a ceramic component. Thus, in Section 6, crack-healing behavior under stress and the resultant strength at the temperature of the crack healing are introduced in detail. Even if all surface cracks were healed completely, embedded flaws such as cracks and pores cannot be healed, because oxygen is necessary for crack healing. Thus, a proof test is necessary for the higher reliability. In Section 7, a detailed explanation of the proof test theory and its usefulness is given. In Section 8, a methodology to increase the through life reliability of ceramic components is explained.

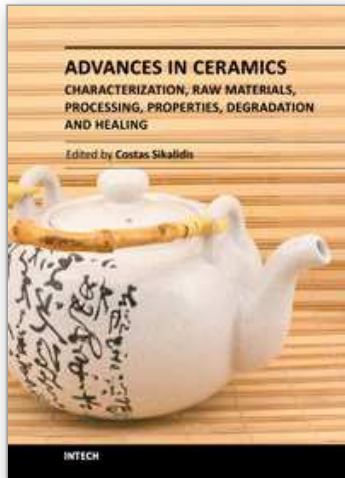
In conclusion, the crack-healing ability of structural ceramics is a very useful technology for higher structural integrity and for reducing the machining and non-destructive inspection costs.

10. References

- Ando, K.; Iwasa, M.; Kim, B.A.; Chu, M.C. & Sato, S. (1993). Effects of crack length, notch root radius and grain size on fracture toughness of fine ceramics. *Fatigue & Fracture of Engineering Materials & Structures*, 16, pp. 995-1006.
- Ando, K.; Ikeda, T.; Sato, S.; Yao, F. & Kobayashi, Y. (1998). A preliminary study on crack healing behaviour of $\text{Si}_3\text{N}_4/\text{SiC}$ composite ceramics. *Fatigue & Fracture of Engineering Materials & Structures*, 21,1,pp.119-122.
- Ando, K.; Furusawa, K.; Chu, M.C.; Hanagata, T.; Tuji, K. & Sato, S. (2001). Crack-healing behavior under stress of mullite/silicon carbide ceramics and the resultant fatigue strength. *Journal of the American Ceramic Society*, 84, 9, pp.2073-2078.
- Ando, K.; Furusawa, K.; Takahashi, K.; Chu, M.C. & Sato, S. (2002a). Crack-healing behavior of structural ceramics under constant and cyclic stress at elevated temperature. *Journal of the Ceramic Society of Japan*, 110, 8, pp.741-747.
- Ando, K., Takahashi, K., Nakayama, S. & Saito, S. (2002b). Crack-Healing Behavior of $\text{Si}_3\text{N}_4/\text{SiC}$ Ceramics under Cyclic Stress and Resultant Fatigue Strength at the Healing Temperature. *Journal of the American Ceramic Society*, 85, 9, pp.2268-2272.
- Ando, K.; Shirai, Y.; Nakatani, M.; Kobayashi, Y. & Sato, S. (2002c). (Crack-healing + proof test): a new methodology to guarantee the structural integrity of a ceramics component. *Journal of the European Ceramic Society*. 22, 1, pp.121-128.

- Ando, K.; Kim, B.S.; Chu, M.C.; Saito, S. & Takahashi, K. (2004). Crack-healing and mechanical behaviour of Al₂O₃/SiC composites at elevated temperature. *Fatigue & Fracture of Engineering Materials & Structures*, 27, 7, pp.533-541.
- Ando, K.; Furusawa, K.; Takahashi, K. & Sato, S. (2005). Crack-healing ability of structural ceramics and a new methodology to guarantee the structural integrity using the ability and proof-test. *Journal of the European Ceramic Society*. 25, 5, pp. 549-558.
- Ando, K.; Takahashi, K.; & Nakao, W. (2009). Self-crack-healing behavior of structural ceramics, In: *Handbook of Nanoceramics and Their Based Nanodevices*, T.Y. Tseng and H.S. Nalwa (Eds.), Vol.1, Chapter 3, 1-26, American Scientific Publishers, Valencia, USA.
- Chou, I. A., Chan, H. M. and Harmer, M. P. (1998), Effect of annealing environment on the crack healing and mechanical behavior of silicon carbide-reinforced alumina nanocomposites. *Journal of the American Ceramic Society*, 81, pp.1203-1208.
- Chu, M.C.; Sato, S.; Kobayashi Y. & Ando, K. (1995). Damage Healing and Strengthening Behavior in Intelligent Mullite/SiC Ceramics. *Fatigue & Fracture of Engineering Materials & Structures*, 18, 9, pp. 1019-1029.
- Houjou, K.; Ando, K. & Takahashi, K. (2010). Crack-healing behaviour of ZrO₂/SiC composite ceramics, *International Journal of Structural Integrity*, 1, 1, pp.73-84.
- Jung, Y.S.; Nakao, W.; Takahashi, K.; Ando, K. & Saito, S. (2008a). Crack-Healing Behavior of Si₃N₄/SiC Composite under Low Oxygen Partial Pressure. *Journal of the Society of Materials Science, Japan*, 57, 11, pp.1132-1137.
- Jung, Y.S.; Guo, Y.; Nakao, W.; Takahashi, K.; Ando, K. & Saito, S. (2008b). Crack-healing behaviour and resultant high-temperature fatigue strength of machined Si₃N₄/SiC composite ceramic. *Fatigue & Fracture of Engineering Materials & Structures*, 31, 1, pp. 2-11.
- Kim, B.S.; Ando, K.; Chu, M.C. & Saito, S. (2003). Crack-healing behavior of monolithic alumina and strength of crack-healed member. *Journal of the Society of Materials Science, Japan*, 52, 6, pp.667-673.
- Kim, Y.W.; Ando, K. & Chu, M.C. (2003). Crack-healing behavior of liquid-phase-sintered silicon carbide ceramics. *Journal of the American Ceramic Society*, 86, 3, pp.465-470.
- Lange, F.F. & Gupta, T.K. (1970). Crack healing by heat treatment. *Journal of the American Ceramic Society*, 53, 1, pp. 54-55.
- Lee, S.K.; Ando, K. & Kim, Y.W. (2005a). Effect of heat treatments on the crack-healing and static fatigue behavior of silicon carbide sintered with Sc₂O₃ and AlN. *Journal of the American Ceramic Society*, 88, 12, pp.3478-3482.
- Lee, S.K.; Ishida, W.; Lee, S.Y.; Nam, K.W. & Ando, K. (2005b). Crack-healing behavior and resultant strength properties of silicon carbide ceramic. *Journal of the European Ceramic Society*, 25, 5, pp.569-576.
- Lee, S.K.; Ono, M.; Nakao, W.; Takahashi, K. & Ando, K. (2005c). Crack-healing behaviour of mullite/SiC/Y₂O₃ composites and its application to the structural integrity of machined components, *Journal of the European Ceramic Society*. 25, 15, pp.3495-3502.
- Nakao, W.; Osada, T.; Yamane, K.; Takahashi, K. & Ando, K. (2005a). Crack-healing mechanism by alumina/SiC particles/SiC whiskers multi-composite, *Journal of The Japan Institute of Metals*, 69, 8, pp.663-666.

- Nakao, W.; Ono, M.; Lee, S.K.; Takahashi, K. & Ando, K. (2005b). Critical crack-healing condition for SiC whisker reinforced alumina under stress. *Journal of the European Ceramic Society*, 25, 16, pp.3649-3655.
- Nakao, W.; Mori, S.; Nakamura, J.; Takahashi, K.; Ando, K. & Yokouchi, M. (2006). Self-crack-healing behavior of mullite/SiC particle/SiC whisker multi-composites and potential use for ceramic springs. *Journal of the American Ceramic Society*, 89, 4, pp.1352-1357.
- Nakao, W.; Takahashi, K. & Ando, K. (2007). Threshold stress during crack-healing treatment of structural ceramics having the crack-healing ability. *Material Letters*, 61, 13, pp.2711-2713.
- Nakao, W.; Takahashi, K. & Ando, K. (2009). Self-healing of surface cracks in structural ceramics, In: *Self-healing Materials*, S.K. Ghosh (Ed.), Chapter 6, 183-217, WILEY-VCH, Weinheim, Germany.
- Nakatani, M.; Sato, S.; Kobayashi, Y. & Ando, K. (2005). A study on crack-healing + proof test to guarantee the structural integrity of ceramic coil springs, *Journal of High Pressure Institute of Japan*, 43, 2, pp.85-91.
- Niihara, K. (1991). New design concept of structural ceramics. *Journal of the Ceramic Society of Japan*. 99, 10, pp.974-982.
- Ono, M.; Nakao, W.; Takahashi, K.; Nakatani, M. & Ando, K. (2007). A new methodology to guarantee the structural integrity of Al₂O₃/SiC composite using crack healing and a proof test, *Fatigue & Fracture of Engineering Materials & Structures*, 30, 7, pp.599-607.
- Osada, T.; Nakao, W.; Takahashi, K.; Ando, K. & Saito, S. (2007). Strength recovery behavior of machined alumina/SiC whisker composite by crack-healing, *Journal of the Ceramic Society of Japan*, 115, 1340, pp.278-284.
- Osada, T.; Nakao, W.; Takahashi, K. & Ando, K. (2009). Kinetics of self-crack-healing of alumina/silicon carbide composite including oxygen partial pressure effect, *Journal of the American Ceramic Society*, 92, 4, pp.864-869.
- Takahashi, K.; Yokouchi, M.; Lee, S.K. & Ando, K. (2003). Crack-healing behavior of Al₂O₃ toughened by SiC whiskers, *Journal of the American Ceramic Society*, 86, 12, pp.2143-2147.
- Takahashi, K.; Ando, K.; Murase, H.; Nakayama, S.; & Saito, S. (2005), Threshold stress for crack-healing of Si₃N₄/SiC and resultant cyclic fatigue strength at the healing temperature. *Journal of the American Ceramic Society*, 88, 3, pp.645-651.
- Takahashi, K.; Uchiide, K.; Kimura, Y.; Nakao, W.; Ando, K. & Yokouchi, M. (2007). Threshold stress for crack healing of mullite reinforced by SiC whiskers and SiC particles and resultant fatigue strength at the healing temperature. *Journal of the American Ceramic Society*, 90, 7, pp.2159-2164.
- Takahashi, K.; Jung, Y.S.; Nagoshi, Y. & Ando, K. (2010). Crack-healing behavior of Si₃N₄/SiC composite under stress and low oxygen pressure, *Materials Science and Engineering A*, 527, 15, pp.3343-3348.
- Thompson, A. M., Chan, H. M., Harmer, M. P. and Cook, R. E. (1995), Crack healing and stress relaxation in Al₂O₃ / SiC "nanocomposites". *Journal of the American Ceramic Society*, 78, pp.567-571.
- Yao, F.; Ando, K.; Chu, M.C. & Sato, S. (2001). Static and cyclic fatigue behaviour of crack-healed Si₃N₄/SiC composite ceramics. *Journal of the European Ceramic Society*, 21, 7, pp.991-997.



Advances in Ceramics - Characterization, Raw Materials, Processing, Properties, Degradation and Healing

Edited by Prof. Costas Sikalidis

ISBN 978-953-307-504-4

Hard cover, 370 pages

Publisher InTech

Published online 01, August, 2011

Published in print edition August, 2011

The current book consists of eighteen chapters divided into three sections. Section I includes nine topics in characterization techniques and evaluation of advanced ceramics dealing with newly developed photothermal, ultrasonic and ion sputtering techniques, the neutron irradiation and the properties of ceramics, the existence of a polytypic multi-structured boron carbide, the oxygen isotope exchange between gases and nanoscale oxides and the evaluation of perovskite structures ceramics for sensors and ultrasonic applications. Section II includes six topics in raw materials, processes and mechanical and other properties of conventional and advanced ceramic materials, dealing with the evaluation of local raw materials and various types and forms of wastes for ceramics production, the effect of production parameters on ceramic properties, the evaluation of dental ceramics through application parameters and the reinforcement of ceramics by fibers. Section III, includes three topics in degradation, aging and healing of ceramic materials, dealing with the effect of granite waste addition on artificial and natural degradation bricks, the effect of aging, micro-voids, and self-healing on mechanical properties of glass ceramics and the crack-healing ability of structural ceramics.

How to reference

In order to correctly reference this scholarly work, feel free to copy and paste the following:

Koji Takahashi, Kotoji Ando and Wataru Nakao (2011). Crack-Healing Ability of Structural Ceramics and Methodology to Guarantee the Reliability of Ceramic Components, *Advances in Ceramics - Characterization, Raw Materials, Processing, Properties, Degradation and Healing*, Prof. Costas Sikalidis (Ed.), ISBN: 978-953-307-504-4, InTech, Available from: <http://www.intechopen.com/books/advances-in-ceramics-characterization-raw-materials-processing-properties-degradation-and-healing/crack-healing-ability-of-structural-ceramics-and-methodology-to-guarantee-the-reliability-of-ceramic>

INTECH
open science | open minds

InTech Europe

University Campus STeP Ri
Slavka Krautzeka 83/A
51000 Rijeka, Croatia
Phone: +385 (51) 770 447
Fax: +385 (51) 686 166
www.intechopen.com

InTech China

Unit 405, Office Block, Hotel Equatorial Shanghai
No.65, Yan An Road (West), Shanghai, 200040, China
中国上海市延安西路65号上海国际贵都大饭店办公楼405单元
Phone: +86-21-62489820
Fax: +86-21-62489821

© 2011 The Author(s). Licensee IntechOpen. This chapter is distributed under the terms of the [Creative Commons Attribution-NonCommercial-ShareAlike-3.0 License](#), which permits use, distribution and reproduction for non-commercial purposes, provided the original is properly cited and derivative works building on this content are distributed under the same license.

IntechOpen

IntechOpen